Journal of Sound and Vibration (1991) **150**(3), 457–484

AN IDENTIFICATION PROBLEM FOR VIBRATING CRACKED BEAMS

M.-H. H. SHEN

Department of Aeronautical and Astronautical Engineering, The Ohio State University, Columbus, Ohio 43210-1276, *U.S.A.*

AND

J. E. TAYLOR

Department of Aerospace Engineering, The University of Michigan, Ann Arbor, Michigan 48109-2125, *U.S.A.*

(*Received* 29 *March* 1990, *and in final form* 2 *November* 1990)

An identification procedure to determine the crack characteristics (location and size of the crack) from dynamic measurements is developed and tested. This procedure is based on minimization of either the "mean-square" or the "max" measure of difference between measurement data (natural frequencies and mode shapes) and the corresponding predictions obtained from the computational model. Necessary conditions are obtained for both formulations. The method is tested for simulated damage in the form of one-side or symmetric cracks in a simply supported Bernoulli–Euler beam. The sensitivity of the solution of damage identification to the values of parameters that characterize damage is discussed.

1. INTRODUCTION

In order to treat the crack identification problem effectively, one should consider the question of what sort of *operating data* information might be most useful for this purpose. The stress state σ_{ij} near a crack tip has the well-known formulation (Irwin [1], and Paris and Sih [2]), $\sigma_{ij}=(K/\sqrt{r})f_{ij}(\theta)$. Here K is the stress intensity factor, r is the distance from the crack tip, and $f_{ij}(\theta)$ is a set of functions of the orientation angle. It follows from the above equation that near a crack tip stresses are concentrated and thus local deformations occur, resulting in a reduction of the bending stiffness locally. In turn, this additional flexibility alters the global dynamics of the structure. In a number of studies (Mayes and Davies [3], Henry and Okah-Avae [4], Cawley and Adams [5], Dimarogonas and Papadopoulos [6], Gudmundson [7], Papadopoulos and Dimarogonas [8], Christides and Barr [9], Shen and Pierre [10, 11], etc.) global dynamical properties of the structure are used as the basis for its crack detection.

The concepts presented in studies mentioned above are concerned mostly with the analysis and determination of the *behavior* of cracked beams (e.g., natural frequencies, mode shapes, strain energy, etc.) given *properties* such as crack lengths or crack ratios, crack positions, etc. The question of the estimation or determination of such *properties* in the case where the *behavior* of the system is known, i.e., the inverse problem, is discussed in this paper.

In the past several years a number of techniques for physical system property identification have been developed (Borg [12], Gel'fand and Levitan [13, 14], Backus and

0022-460X/91/210457+28 $03.00/0

Gilbert [15], Newton [16], Barcilon [17–20], McLaughlin [21–23]). Some of these techniques have been applied to structural problems by Barcilon [20, 24], McLaughlin [22, 23], Gladwell [25–27] and Gladwell *et al.* [28]. Most of these treatments involve the determination of material properties from natural frequencies, and they emphasize the existence, uniqueness and methods for determination of properties (termed "reconstruction").

Inverse problems in one-dimensional vibrating continuous structures can be separated into two categories: the longitudinal or simple torsional vibrations which are governed by a second order differential equation, and the bending vibration governed by a fourth order system. In the former, the goal is to recover the coefficients from information about the solutions of a second order equation or the solution of a Sturm–Liouville equation.

The inverse problem for the free flexural vibration of a Bernoulli Euler beam began with the work of Barcilon [18, 19] and later was improved by McLaughlin [21, 22, 29, 30], and analyzed by Gladwell [27] and Gladwell *et al.* [28]. Three basic questions were fully discussed in these papers. First, how many and what kind of spectral data are needed to identify the beam's properties (cross-section area, $A(x)$, and second moment of area, $I(x)$)? In other words: What are the requirements of the spectral data in order to determine the properties uniquely? Three spectra corresponding to three different end conditions (clamped–free, clamped–pinned and clamped–sliding) were suggested by Barcilon [18, 19]. These results were further confirmed by Gladwell *et al.* [28]. Secondly, what are necessary and sufficient conditions for the existence of the results from the inverse process? Barcilon [24] attacked this question by observing the response of a vibrating cantilevered beam, but it was not fully answered until Gladwell's subsequent investigation [27]. Gladwell derived a set of inequalities which were used to find a limiting region for the spectral data. If the given spectral data are selected within in this region, a realizable beam can be constructed. Thirdly, what procedure properly reconstructs the beam? This question was initiated by Barcilon [20], and a standard procedure for reconstructing a Bernoulli–Euler beam was completed by McLaughlin a few years later [22]. The basic concept of this procedure was an extension of the ideas of his previous work (McLaughlin [30]) for determining the coefficient of a second order system. This procedure has been applied successfully to many inverse problems associated with the Bernoulli–Euler beam model (Gladwell [27] and Gladwell *et al.* [28]).

To summarize, each of the continuous systems discussed in the studies mentioned above can be formulated as a fourth order linear eigenvalue problem with separable boundary conditions. The inverse problem to be considered is to recover the coefficients in the differential equation and boundary conditions from knowledge of the eigenvalues or related spectral data.

The free flexural vibrations of slender beams with one pair of symmetric cracks may be modelled via equation (7), $(EIQw'')'' + \rho A\ddot{w} = 0$, as described in Shen and Pierre [10]. Here the modified second moment of area, IQ, is dependent on not only the beam's longitudinal co-ordinate, x, but also on the crack position, xc, and crack ratio (crack length), cr. The inverse problem for these equations, i.e., the reconstruction of $I(x)Q(x, xc, cr)$ from spectral (i.e., natural frequencies and mode shapes changes) data, will be the main subject of this paper. Specifically, the problem of how to obtain a best approximation of the structural properties of cracked (damaged) beams is treated in what follows.

The aforementioned conventional techniques are not applicable in their given form to identify the cracked beam's properties, crack position xc and crack ratio cr, from its natural frequencies. First, most of these techniques deal with the simple Bernoulli–Euler beam model in a way that requires that $A(x)$ and $I(x)$ are twice continuously differentiable. Hence, it is impossible to apply these techniques directly to the present cracked beam model since IQ has only first order continuity (see Shen and Pierre [10]). Also, for the

previous techniques it is assumed that complete spectral data are known exactly and are collected on the basis of at least three different structural or support configurations. Thus, for practical reasons the detection of cracks based on data for a given, unique vibrating structure cannot be accomplished using such methods.

The methods described in this paper are suitable for use as on-line non-intrusive damage detection techniques of a vibrating beam. For the purpose of this study, the beam's damage is characterized in the mathematical model by the parameters cr and xc, defined as $(d-h)/d$ and x_c/l, respectively (see Figure 1). The idea of this procedure is related to methods of

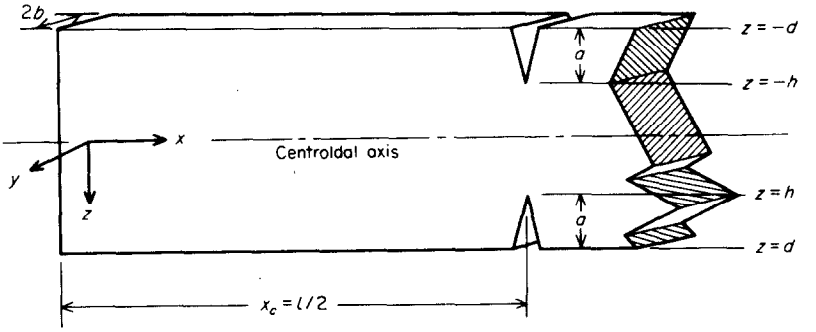

Figure 1. Geometry of a simply supported beam containing a pair of symmetric edge cracks at mid-span, $xc = 1/2$.

structural optimization. Specifically, the structural damage is identified in a way to minimize one or another measure of the difference between a set of data (measurements) T_d, and the corresponding values for dynamic response M_d obtained by analysis of a model for the damaged beam. This may be expressed symbolically as the following optimization problem:

$$\min_{xc,cr} norm(T_d - M_d). \tag{1}$$

Naturally, the minimization represented here is constrained by the equations which model the physical system. Moreover, as indicated in the discussion by Shen and Pierre [10, 11], one can note that the more model information used for crack detection, the more accurate and reliable the result that can be achieved. For our purposes, the objective of equation (1) is formulated based on a certain set of specific modes; specifically the first M modes are considered in the inverse procedure. Accordingly, it should be understood that the norm of equation (1) reflects all modal data in the set. Some questions related to the selection of proper modes to be used in the optimization process are discussed in section 2.

Among possible explicit forms for the problem of equation (1), the two corresponding to the mean-square measure and the "max" measure of the norm are to be examined in detail. The problem statements corresponding to each of these two versions of the norm are expressed in variational form in section 2. The development is expressed for the vibrating simply supported beam with a pair of cracks. This formulation is interpreted to obtain a set of necessary conditions. Methods for the computational treatment to these problems are presented in section 3.

These inverse vibrating beam problems are investigated numerically in section 4. The effectiveness and limitations of the computational methods are discussed there.

2. PROBLEM FORMULATION FOR THE IDENTIFICATION OF A CRACKED BEAM

In this section, variational formulations for the identification of a cracked beam with one pair of symmetric cracks are presented. The mean square differences between measured and modelled values of frequency and mode shape are employed as the objective function in one of the formulations. In other words, the inverse process seeks to determine the crack parameters, xc and cr, in the mathematical model to minimize the mean square difference between the test data and analytical predictions. As noted above, the identification problem can be treated as well in the form of a min–max problem; this formulation is presented in section 2.2. Both problem formulations are presented in forms consistent with having the beam deflection data stated either in discrete or continuous form.

2.1. MEAN SQUARE ERROR FORM OF PROBLEM STATEMENT

2.1.1. *Discrete deflection data*

In the first treatment of this problem, it is assumed that the testing information (data) is provided from certain test points distributed over the structure. This data is comprised of frequency and mode shape information associated with the lower several response modes.

For a simply supported uniform beam containing one pair of symmetric cracks (see Figure 1), the problem of optimization in crack detection can be expressed, in terms of comparisons between modelled response and test data, as

$$\min_{cr,xc} [norm(\omega_{t\alpha}^2 - \omega_\alpha^2,\, w_{t\alpha}(x_{tm}) - w_\alpha(x_{tm}))], \tag{2}$$

subject to constraints that define the beam response w_α (i.e., the equations for free vibration), and which prescribe appropriate normalization of w_α and test data $w_{t\alpha}$.

Here $cr=(d-h)/d$ represents crack ratio (a measure of crack depth), and xc identifies crack position (see Figure 1). Also, the objective function measure of differences between measured and modelled values of deflection and frequency in equation (2) is stated for present purposes in the form:

$$norm(\omega_{t\alpha}^2 - \omega_\alpha^2,\, w_{t\alpha} - w_\alpha) = \left(\sum_{\alpha=1}^{M} [(\omega_{t\alpha}^2 - \omega_\alpha^2)^2 + \sum_{m=1}^{T} (w_{t\alpha}(x_{tm}) - w_\alpha(x_{tm}))^2] \right)^{1/2}, \tag{3}$$

where ω_α and w_α represent the natural frequency and mode shape of the αth bending free vibration mode, M is the number of modes for which test information is available, and, once again, the corresponding test data are symbolized by $\omega_{t\alpha}$ and $w_{t\alpha}$. Here x_{tm} ($m=1, 2, \ldots, T$) locates the mth out of T measurement stations, respectively. The measures $w_{t\alpha}$ and w_α that appear in the norm must be normalized on a common basis in order to facilitate comparison between the data and model values. Since $w_{t\alpha}$ is known only at points along the beam, the model deflection is normalized as follows.

Suppose that $\eta_{a\alpha}$ is defined as

$$\eta_{a\alpha} = \frac{x_1}{2} w_{t\alpha}^2 \Big|_0 + \sum_{m=2}^{T-1} w_{t\alpha}^2 \Big|_{x_{tm}} \Delta x_{tm} + \frac{l - x_{T-1}}{2} w_{t\alpha}^2 \Big|_l. \tag{4}$$

Then, for consistency, the model deflection w_α is required to satisfy the similar expression

$$\eta_{a\alpha} = \frac{x_1}{2} w_\alpha^2 \Big|_0 + \sum_{m=2}^{T-1} w_\alpha^2 \Big|_{x_{tm}} \Delta x_{tm} + \frac{l - x_{T-1}}{2} w_\alpha^2 \Big|_l, \tag{5}$$

where $\Delta x_{tm} = \frac{1}{2}[x_{t(m+1)} - x_{t(m-1)}]$. Note that in the case of a simply supported beam, where

the displacements w_α vanish at the two end boundaries, equations (4) and (5) can be rewritten as

$$\eta_{\alpha\alpha} = \sum_{m=2}^{T-1} w_{t\alpha}^2 \Big|_{x_{tm}} \Delta x_{tm} \qquad \text{and} \qquad \eta_{\alpha\alpha} = \sum_{m=2}^{T-1} w_\alpha^2 \Big|_{x_{tm}} \Delta x_{tm}, \tag{6, 7}$$

respectively. For equal measured span, $\Delta x_{tm} = l/(T-1)$, equation (7) is reformulated as

$$\eta_{\alpha\alpha} \frac{(T-1)}{l} = \sum_{m=2}^{T-1} w_\alpha^2 \Big|_{x_{tm}}. \tag{8}$$

In order to relate w_α defined by equations (5–8) to the usual normalization, consider $\hat{w}_\alpha$, where $\int_0^l \hat{w}_\alpha^2 \, dx = 1$; $\alpha = 1, 2, \ldots, M$. Then for $w_\alpha = C_\alpha \hat{w}_\alpha$,

$$\int_0^l w_\alpha^2 \, dx = \int_0^l C_\alpha^2 \hat{w}_\alpha^2 \, dx = C_\alpha^2. \tag{9}$$

The values $\eta_{\alpha\alpha}$ and C_α are related. For the case represented via equation (7) as an example,

$$\sum_{m=2}^{T-1} \hat{w}_\alpha^2 \Big|_{x_{tm}} \Delta x_{tm} = \eta_{\alpha\alpha} / C_\alpha^2. \tag{10}$$

It is noted from equation (7) that $\eta_{\alpha\alpha}$ is a function of the number T of measurements stations. Taking the normalization of $\hat{w}_\alpha$ into account, equation (10) provides

$$\lim_{T \to \infty} \eta_{\alpha\alpha} = C_\alpha^2. \tag{11}$$

This property can be useful to verify the accuracy of computations.

The symbol Φ is introduced to represent the square of the norm given in equation (3). The identification problem now can be stated:

$$\min_{cr, xc} \Phi, \tag{12}$$

subject to

$$\int_0^l \{EIQ(w_\alpha''(x))^2 - \omega_\alpha^2 \rho A w_\alpha^2(x)\} \, dx = 0, \tag{13}$$

$$\sum_{m=2}^{T-1} (w_\alpha(x_{tm}) w_\beta(x_{tm})) \Delta x_{tm} - \eta_{\alpha\beta} = 0, \tag{14}$$

$$(cr + \underline{a} xc) - R \leqslant 0, \qquad \underline{cr} \leqslant cr \leqslant \overline{cr}, \qquad \underline{xc} \leqslant xc \leqslant \overline{xc}, \tag{15–17}$$

where $\alpha, \beta = 1, \ldots, M$, $\underline{a}$ is a weighting factor on the cr and xc, R represents the upper bound on value $cr + \underline{a} xc$, and $\overline{xc}$, $\underline{xc}$ and $\overline{cr}$, $\underline{cr}$ represent the upper and lower bounds of the crack (damage) parameters xc and cr, respectively. (Note that both upper and lower bounds on the variables cr and xc are necessary in the present problem.) Since w_α comprise an orthonormal set, $\eta_{\alpha\beta}$ defined as in equation (7) satisfies:

$$\lim_{T \to \infty} \eta_{\alpha\beta} = 0 \qquad \text{for } \alpha \neq \beta.$$

The effect of cracks on the structural properties of the beam is reflected by the factor Q in equation (13), as described for symmetric surface cracks in Shen and Pierre [10] and in Christides and Barr [9], and for the single surface crack problem in Shen and Pierre [11].

In other words, the optimization parameters xc and cr cited in equation (12) enter the problem via Q.

According to K–K–T (Kurash–Kuhn–Tucker), necessary conditions for the optimization problem equations (12–17) there exist Lagrange multipliers λ_α, $\Lambda_{\alpha\beta}$ and Γ_k which satisfy the following equations (the notation "$|_*$" refers to solution points):

$$\lambda_\alpha > 0, \qquad \Lambda_{\alpha\beta} > 0, \qquad \Gamma_1[(cr + \underline{a}xc) - R]|_* = 0, \qquad [\Gamma_2(\underline{cr} - cr)]|_* = 0, \quad (18, 19)$$

$$[\Gamma_3(xc - \overline{xc})]|_* = 0, \qquad [\Gamma_4(\underline{xc} - xc)]|_* = 0, \qquad [\Gamma_5(cr - \overline{cr})]|_* = 0. \quad (20\text{–}22)$$

The solution must satisfy the following three equations as well:

$$[2(\omega_{t\alpha}^2 - \omega_\alpha^2) + \lambda_\alpha \rho A C_\alpha^2]|_* = 0, \quad (23)$$

$$[(EIQw_\alpha''(x))'' - \omega_\alpha^2 \rho A w_\alpha(x)]|_* = 0, \qquad x_{tm} < x < x_{t(m+1)}, \quad (24)$$

$$\sum_{m=2}^{T-1} \Bigg\{ -2(w_{t\alpha}(x) - w_\alpha(x)) + 2\Lambda_{\alpha\alpha} w_\alpha(x) + \sum_{\beta=1}^{\alpha-1} \Lambda_{\alpha\beta} w_\beta(x) + \sum_{\beta=\alpha+1}^{M} \Lambda_{\alpha\beta} w_\beta(x) \Big] \Delta x_{tm} + 2\lambda_\alpha [(EIQw_\alpha''(x))'' - \omega_\alpha^2 \rho A w_\alpha(x)] \Bigg\} |_{x = x_{tm}}|_* = 0. \quad (25)$$

Note that the above equation of motion (24) is valid interval by interval over the span of the structure.

Finally, the conditions for stationarity of Φ with respect to the optimization variables cr and xc (i.e., the optimality conditions) are:

$$\left[\sum_{\alpha=1}^{M} \lambda_\alpha \left(EI \int_0^l \frac{\partial Q}{\partial cr} (w_\alpha''(x))^2 \, dx \right) + \Gamma_1 - \Gamma_2 + \Gamma_5 \right]_* = 0, \quad (26)$$

$$\left[\sum_{\alpha=1}^{M} \lambda_\alpha \left(EI \int_0^l \frac{\partial Q}{\partial xc} (w_\alpha''(x))^2 \, dx \right) + \Gamma_1 \underline{a} + \Gamma_3 - \Gamma_4 \right]_* = 0. \quad (27)$$

2.1.2. *Continuous testing deflection data*

The problem statement and associated necessary conditions are rewritten here for the situation in which the testing information is provided in continuous form, i.e., along the entire structure. Thus the above crack identification problem statement is modified by replacing each summation on m with integration over the span variable. The resulting problem statement is

$$\min_{cr, xc} \sum_{\alpha=1}^{M} \left[(\omega_{t\alpha}^2 - \omega_\alpha^2)^2 + \int_0^l (w_{t\alpha}(x) - w_\alpha(x))^2 \, dx \right], \quad (28)$$

subject to

$$\int_0^l \{EIQ(w_\alpha''(x))^2 - \omega_\alpha^2 \rho A w_\alpha^2(x)\} \, dx = 0, \quad (29)$$

$$\int_0^l w_\alpha(x) w_\beta(x) \, dx - C_\alpha^2 \delta_{\alpha\beta} = 0, \quad (30)$$

$$(cr + \underline{a}xc) - R \leqslant 0, \qquad \underline{cr} \leqslant cr \leqslant \overline{cr}, \qquad \underline{xc} \leqslant xc \leqslant \overline{xc}, \quad (31\text{–}33)$$

where $\alpha, \beta = 1, \ldots, M$ and C_α is defined in equation (9).

The necessary conditions for the optimal solution, comparable to equations (18–27), are

$$\lambda_\alpha > 0, \qquad \Lambda_{\alpha\beta} > 0, \qquad \Gamma_1[(cr + \underline{a}xc) - R]\,|_* = 0, \qquad [\Gamma_2(\underline{cr} - cr)]\,|_* = 0, \quad (34, 35)$$

$$[\Gamma_3(xc - \overline{xc})]\,|_* = 0, \qquad [\Gamma_4(\underline{xc} - xc)]\,|_* = 0, \qquad [\Gamma_5(cr - \overline{cr})]\,|_* = 0, \quad (36\text{–}38)$$

$$[2(\omega_{i\alpha}^2 - \omega_\alpha^2) + \lambda_\alpha \rho A C_\alpha^2]\,|_* = 0, \quad (39)$$

$$\Big[2\lambda_\alpha (EIQw_\alpha'(x))'' - 2(w_{i\alpha}(x) - w_\alpha(x)) + 2\Lambda_{\alpha\alpha} w_\alpha(x) + \sum_{\beta=1}^{\alpha-1} \Lambda_{\alpha\beta} w_\beta(x) + \sum_{\beta=\alpha+1}^{M} \Lambda_{\alpha\beta} w_\beta(x)\Big]\Big|_* = 0, \qquad 0 < x < l, \quad (40)$$

$$\left[\sum_{\alpha=1}^{M} \lambda_\alpha \left(EI \int_0^l \frac{\partial Q}{\partial cr} (w_\alpha''(x))^2 \, dx\right) + \Gamma_1 - \Gamma_2 + \Gamma_5\right]\Big|_* = 0, \quad (41)$$

$$\left[\sum_{\alpha=1}^{M} \lambda_\alpha \left(EI \int_0^l \frac{\partial Q}{\partial xc} (w_\alpha''(x))^2 \, dx\right) + \Gamma_1 \underline{a} + \Gamma_3 - \Gamma_4\right]\Big|_* = 0. \quad (42)$$

The system of equations for this latter version can be reduced as follows. In order to determine the Lagrangian multipliers $\Lambda_{\alpha\alpha}$, first multiply equation (40) by w_α, integrate by parts and apply the boundary conditions, and use equations (29) and (30). The result for $\Lambda_{\alpha\alpha}$ is simply

$$\Lambda_{\alpha\alpha} = -\lambda_\alpha \omega_\alpha^2 \rho A + \frac{1}{C_\alpha^2} \int_0^l w_{i\alpha} w_\alpha \, dx - 1. \quad (43)$$

To determine the remaining components of $\Lambda_{\alpha\beta}$ (i.e., those associated with $\alpha \neq \beta$), we first write equation (40) with index α replaced by γ. Then, multiply this equation by w_α and equation (40) by w_γ, integrate both equations by parts using the boundary conditions, assume that $\alpha \neq \gamma$, and apply equation (30). Subtracting and adding the two resulting equations yields

$$\Lambda_{\alpha\gamma} = -(\lambda_\alpha + \lambda_\gamma) \int_0^l EIQ w_\alpha'' w_\gamma'' \, dx, \qquad \alpha \neq \gamma, \quad (44)$$

$$(\lambda_\alpha - \lambda_\gamma) \int_0^l EIQ w_\alpha'' w_\gamma'' \, dx = 0, \qquad \alpha \neq \gamma. \quad (45)$$

From equations (44) and (45), we can see that

$$\Lambda_{\alpha\gamma} = 0, \qquad \alpha \neq \gamma, \qquad \alpha = 1, \ldots, M. \quad (46)$$

Here, for simplicity, we assume that all the design constraints are not critical, whereby all the corresponding Γ_i are zero. Then the necessary conditions of equations (34–42) can be reduced to

$$\left\{2 \frac{(\omega_{i\alpha}^2 - \omega_\alpha^2)}{\rho A C_\alpha^2} [(EIQw_\alpha'(x))'' - \omega_\alpha^2 \rho A w_\alpha(x)] + \frac{w_\alpha}{C_\alpha^2} \int_0^l w_{i\alpha} w_\alpha \, dx - w_{i\alpha}\right\}\Big|_* = 0, \qquad 0 < x < l, \quad (47)$$

$$\left[\sum_{\alpha=1}^{M}\frac{(\omega_{l\alpha}^2-\omega_\alpha^2)}{\rho AC_\alpha^2}\int_0^l\frac{\partial Q}{\partial cr}(w_\alpha'')^2\,dx)\right]\Big|_*=0, \tag{48}$$

$$\left[\sum_{\alpha=1}^{M}\frac{(\omega_{l\alpha}^2-\omega_\alpha^2)}{\rho AC_\alpha^2}\int_0^l\frac{\partial Q}{\partial xc}(w_\alpha'')^2\,dx)\right]\Big|_*=0. \tag{49}$$

2.2. MIN MAX PROBLEM STATEMENT

The crack identification problem can be stated in min–max form which corresponds to the goal to minimize the largest value among the set of measures of the difference between test data and corresponding values predicted from the model (the set is indicated by curly brackets). This is expressed as

$$\min_{cr,xc}\left[\max_{\alpha}\{\omega_{l\alpha}^2-\omega_\alpha^2,\, w_{t\alpha}(x_{tm})-w_\alpha(x_{tm})\}\right], \tag{50}$$

subject to the constraints listed as equations (13–17) of the prior formulation. As was indicated by Taylor and Bendsøe [31], this min–max problem can be interpreted as a simple scalar minimization problem, corresponding to minimization of a bound on all elements of the criterion set.

Introducing the symbol Ψ for this bound, the min–max problem is restated in the form

$$\min_{cr,xc}(\Psi), \tag{51}$$

subject to

$$\left[(\omega_{l\alpha}^2-\omega_\alpha^2)^2+\sum_{m=1}^{T}(w_{t\alpha}(x_{tm})-w_\alpha(x_{tm}))^2\right]-\Psi\leqslant 0, \tag{52}$$

for all $\alpha=1,2,\ldots,M$,

$$\int_0^l[EIQ(w_\alpha''(x))^2-\omega_\alpha^2\rho Aw_\alpha^2(x)]\,dx=0, \tag{53}$$

$$\sum_{m=1}^{K}(w_\alpha(x_{tm})w_\beta(x_{tm}))\Delta x_{tm}-\eta_{\alpha\beta}=0, \tag{54}$$

for all $\alpha,\beta=1,2,\ldots,M$, and

$$(cr+\underline{a}xc)-R\leqslant 0, \qquad \underline{cr}\leqslant cr\leqslant\overline{cr}, \qquad \underline{xc}\leqslant xc\leqslant\overline{xc}. \tag{55–57}$$

Here again the analysis associated with this optimization problem is to be considered. According to the necessary K–K–T conditions, there exist Lagrange multipliers λ_α, μ_α, $\Lambda_{\alpha\beta}$ and Γs which satisfy the following equations:

$$\lambda_\alpha>0, \qquad \Lambda_{\alpha\beta}>0, \qquad \sum_{\alpha=1}^{M}\mu_\alpha=1, \tag{58}$$

$$\Gamma_1[(cr+\underline{a}xc)-R]\,|_*=0, \qquad [\Gamma_2(\underline{cr}-cr)]\,|_*=0, \tag{59, 60}$$

$$[\Gamma_3(xc-\overline{xc})]\,|_*=0, \qquad [\Gamma_4(\underline{xc}-xc)]\,|_*=0, \qquad [\Gamma_5(cr-\overline{cr})]\,|_*=0, \tag{61–63}$$

$$[\mu_\alpha[(\omega_{l\alpha}^2-\omega_\alpha^2)^2+\sum_{m=1}^{T}(w_{t\alpha}(x_{tm})-w_\alpha(x_{tm}))^2]-\Psi]\,|_*=0, \tag{64}$$

$$[2\mu_\alpha(\omega_{l\alpha}^2-\omega_\alpha^2)+\lambda_\alpha\rho AC_\alpha^2]\,|_*=0. \tag{65}$$

Additional conditions for stationarity are:

$$[(EIQw''_\alpha(x))'' - \omega_\alpha^2 \rho A w_\alpha(x)]\,|_* = 0, \qquad x_{tm} < x < x_{t(m+1)}, \tag{66}$$

$$\sum_{m=2}^{T-1} \left\{ -2\mu_\alpha(w_{t\alpha}(x) - w_\alpha) + \left[2\Lambda_{\alpha\alpha} w_\alpha(x) + \sum_{\beta=1}^{\alpha-1} \Lambda_{\alpha\beta} w_\beta(x) + \sum_{\beta=\alpha+1}^{M} \Lambda_{\alpha\beta} w_\beta(x) \right] \Delta x_{tm} \right.$$

$$\left. + 2\lambda_\alpha[(EIQw''_\alpha(x))'' - \omega_\alpha^2 \rho A w_\alpha(x)] \right\} \Big|_{x = x_{tm}} \Big|_* = 0, \tag{67}$$

as well as the optimality conditions:

$$\left[\sum_{\alpha=1}^{M} \lambda_\alpha \left(EI \int_0^l \frac{\partial Q}{\partial cr} (w''_\alpha(x))^2 \, dx \right) + \Gamma_1 - \Gamma_2 + \Gamma_5 \right] \Big|_* = 0, \tag{68}$$

$$\left[\sum_{\alpha=1}^{M} \lambda_\alpha \left(EI \int_0^l \frac{\partial Q}{\partial xc} (w''_\alpha(x))^2 \, dx \right) + \Gamma_1 \underline{a} + \Gamma_3 - \Gamma_4 \right] \Big|_* = 0. \tag{69}$$

Assume that M Lagrangian multipliers μ_α are greater than zero, which is the same as assuming that all M modes are "active" in the solution. For simplicity, let us assume also that all the design constraints of equations (59–63) are inactive; then all the corresponding Γ_k are zero. In this case the necessary conditions become:

$$\sum_{\alpha=1}^{M} \mu_\alpha = 1, \tag{70}$$

$$\mu_\alpha[(\omega_{t\alpha}^2 - \omega_\alpha^2)^2 + \sum_{m=1}^{T} (w_{t\alpha}(x_{tm}) - w_\alpha(x_{tm}))^2] - \Psi\,|_* = 0, \tag{71}$$

$$[2\mu_\alpha(\omega_{t\alpha}^2 - \omega_\alpha^2) + \lambda_\alpha \rho A C_\alpha^2]\,|_* = 0, \tag{72}$$

$$[(EIQw''_\alpha(x))'' - \omega_\alpha^2 \rho A w_\alpha(x)]\,|_* = 0, \qquad x_{tm} < x < x_{t(m+1)}, \tag{73}$$

$$\sum_{m=2}^{T-1} \left\{ -2\mu_\alpha(w_{t\alpha}(x) - w_\alpha(x)) + \left[2\Lambda_{\alpha\alpha} w_\alpha(x) + \sum_{\beta=1}^{\alpha-1} \Lambda_{\alpha\beta} w_\beta(x) + \sum_{\beta=\alpha+1}^{M} \Lambda_{\alpha\beta} w_\beta(x) \right] \Delta x_{tm} \right.$$

$$\left. + 2\lambda_\alpha[(EIQw''_\alpha(x))'' - \omega_\alpha^2 \rho A w_\alpha(x)] \right\} \Big|_{x = x_{tm}} \Big|_* = 0. \tag{74}$$

The optimality conditions are simplified as a result, from equations (68) and (69) to:

$$\left[\sum_{\alpha=1}^{M} \lambda_\alpha (EI \int_0^l \frac{\partial Q}{\partial cr} (w''_\alpha(x))^2 \, dx) \right] \Big|_* = 0, \tag{75}$$

$$\left[\sum_{\alpha=1}^{M} \lambda_\alpha (EI \int_0^l \frac{\partial Q}{\partial xc} (w''_\alpha(x))^2 \, dx) \right] \Big|_* = 0. \tag{76}$$

2.2.1. *Continuous testing deflection data*

As was done above for the mean square criterion version, here too the min-max form of problem statement is expressed again, this time as it would be written to accommodate the test data appearing in continuous form. This problem statement can be written as follows:

$$\min_{cr, xc} (\Psi), \tag{77}$$

subject to

$$\left[(\omega_{t\alpha}^2-\omega_\alpha^2)^2+\int_0^l (w_{t\alpha}(x)-w_\alpha(x))^2\right]-\Psi\leqslant 0, \tag{78}$$

$$\int_0^l \{EIQ(w_\alpha''(x))^2-\omega_\alpha^2\rho A w_\alpha^2(x)\}\,dx=0, \tag{79}$$

$$\int_0^l w_\alpha(x)w_\beta(x)\,dx-C_\alpha^2\delta_{\alpha\beta}=0, \tag{80}$$

$$[cr+xc\underline{a}-R]\leqslant 0, \qquad \underline{cr}\leqslant cr\leqslant \overline{cr}, \qquad \underline{xc}\leqslant xc\leqslant \overline{xc}. \tag{81-83}$$

Again, according to the necessary K–K–T conditions we obtain

$$\lambda_\alpha>0, \qquad \Lambda_{\alpha\beta}>0, \qquad \sum_{\alpha=1}^{M}\mu_\alpha=1, \tag{84}$$

$$\Gamma_1[(cr+\underline{a}xc)-R]\,|_*=0, \qquad [\Gamma_2(\underline{cr}-cr)]\,|_*=0, \tag{85, 86}$$

$$[\Gamma_3(xc-\overline{xc})]\,|_*=0, \qquad [\Gamma_4(\underline{xc}-xc)]\,|_*=0, \qquad [\Gamma_5(cr-\overline{cr})]\,|_*=0, \tag{87-89}$$

$$\mu_\alpha[(\omega_{t\alpha}^2-\omega_\alpha^2)^2-\Psi)]\,|_*=0, \tag{90}$$

$$[2\mu_\alpha(\omega_{t\alpha}^2-\omega_\alpha^2)+\lambda_\alpha\rho AC_\alpha^2]\,|_*=0, \tag{91}$$

along with

$$\Bigg[2\lambda_\alpha[(EIQw_\alpha''(x))''-\omega_\alpha^2\rho A w_\alpha(x)]-2(w_{t\alpha}(x)-w_\alpha(x)) + 2\Lambda_{\alpha\alpha}w_\alpha(x)+\sum_{\beta=1}^{\alpha-1}\Lambda_{\alpha\beta}w_\beta(x)+\sum_{\beta=\alpha+1}^{M}\Lambda_{\alpha\beta}w_\beta(x)\Bigg]\Bigg|_*=0, \qquad 0<x<l, \tag{92}$$

and the (optimality) conditions:

$$\left[\sum_{\alpha=1}^{M}\lambda_\alpha\left(EI\int_0^l\frac{\partial Q}{\partial cr}(w_\alpha''(x))^2\,dx\right)+\Gamma_1-\Gamma_2+\Gamma_5\right]\Bigg|_*=0, \tag{93}$$

$$\left[\sum_{\alpha=1}^{M}\lambda_\alpha\left(EI\int_0^l\frac{\partial Q}{\partial xc}(w_\alpha''(x))^2\,dx\right)+\underline{a}\Gamma_1+\Gamma_3-\Gamma_4\right]\Bigg|_*=0. \tag{94}$$

Here again, for simplicity, it is assumed that all the design constraints are not critical; then all the corresponding Γ_i have the value zero. Therefore, the necessary conditions become:

$$\sum_{\alpha=1}^{M}\mu_\alpha=1, \tag{95}$$

$$\left\{2\frac{\mu_\alpha\Psi}{\rho AC_\alpha^2(\omega_{t\alpha}^2-\omega_\alpha^2)}[(EIQw_\alpha''(x))''-\omega_\alpha^2\rho A w_\alpha(x)]+\frac{w_\alpha}{C_\alpha^2}\int_0^l w_{t\alpha}w_\alpha\,dx-w_{t\alpha}\right\}\Bigg|_*=0, \quad 0<x<l, \tag{96}$$

$$\left[\sum_{\alpha=1}^{M} \frac{\mu_\alpha \Psi}{\rho A C_\alpha^2(\omega_{t\alpha}^2-\omega_\alpha^2)}\left(EI\int_0^l \frac{\partial Q}{\partial cr}(w_\alpha''(x))^2\,dx\right)\right]\Bigg|_* = 0, \tag{97}$$

$$\left[\sum_{\alpha=1}^{M} \frac{\mu_\alpha \Psi}{\rho A C_\alpha^2(\omega_{t\alpha}^2-\omega_\alpha^2)}\left(EI\int_0^l \frac{\partial Q}{\partial xc}(w_\alpha''(x))^2\,dx\right)\right]\Bigg|_* = 0. \tag{98}$$

3. COMPUTATIONAL ASPECTS

In order to identify the crack ratio cr and the crack position xc the necessary conditions obtained in the previous section may be solved. It is recalled that certain of these necessary conditions must to be solved for each test span, the "span" being the distance between the test points. It is imperative that the crack identification process be achieved in an efficient manner, to ensure that the method is feasible with respect to the computing time required. Fortunately, there are several well established numerical methods that can be applied directly to the crack identification problems. Therefore, in the present study, these numerical algorithms of optimization are used to achieve the identification; i.e., to obtain solutions for identification problems. Nevertheless, prior to performing the minimization process, it is necessary to reformulate the problem statements presented in the previous sections into a form suitable for the computational treatment.

3.1. THE PROBLEM FORMULATION FOR THE NUMERICAL METHOD: MEAN SQUARE CRITERION

The purpose in this subsection is to re-state the inverse cracked beam problem with mean square criterion, equations (12–17), in the following form that is more convenient for computational purposes. With the introduction of symbols ξ and Υ for convenience, the statement becomes:

$$\min_{\mathbf{x}_1} \sum_{\alpha=1}^{M}\left[(\xi_{t\alpha}-\xi_\alpha)^2+\sum_{m=1}^{T}(w_{t\alpha}(x_{tm})-w_\alpha(x_{tm}))^2\right], \tag{99}$$

subject to

$$\left[\alpha^4 Q\sum_{m=1}^{T}(w_\alpha(x_{tm}))^2-\xi_\alpha\sum_{m=1}^{T}(w_\alpha(x_{tm}))^2\right]\Delta x_{tm}-\Upsilon_\alpha=0, \tag{100}$$

$$\sum_{m=2}^{T-1}(w_\alpha(x_{tm})w_\beta(x_{tm}))\Delta x_{tm}-\eta_{\alpha\beta}=0, \tag{101}$$

$$0\leqslant cr\leqslant 1, \qquad 0\leqslant xc\leqslant 1, \tag{102, 103}$$

where $\alpha, \beta = 1, \ldots, M$, variable vector $\mathbf{x}_1 = \{cr, xc, \xi_\alpha, w_\alpha(x_{tm})\}$, and where

$$\xi_\alpha = \frac{\omega_\alpha^2 l^4 \rho A}{EI\pi^4}, \tag{104}$$

and

$$\Upsilon_\alpha = \left[\alpha^4 Q\sum_{m=1}^{T}(w_{t\alpha}(x_{tm}))^2-\xi_\alpha\sum_{m=1}^{T}(w_{t\alpha}(x_{tm}))^2\right]\Delta x_{tm}. \tag{105}$$

The possibility that the testing mode shapes w_t are provided in the form of continuous functions is also considered. It has been shown in reference [10] that of the deflection

shape w_α of a cracked beam was approximated successfully through the use of the Fourier series. Hence, in a similar manner, it is supposed here that both model and testing mode shapes in the formulation of crack identification can be expressed as

$$w_\alpha(x) = \sum_{i=1}^{N} a_{\alpha i} \sin(i\pi x/l), \qquad w_{t\alpha}(x) = \sum_{i=1}^{N} a_{t\alpha i} \sin(i\pi x/l). \tag{106, 107}$$

The means to determine values for coefficients $a_{\alpha i}$ and $a_{t\alpha i}$ are not considered here.

Substituting equations (106) and (107) into the second term of equation (28), the equation representing the criterion in which testing information is presented in continuous form yields

$$\sum_{i=1}^{N} (a_{t\alpha i} - a_{\alpha i})^2 \int_0^l \sin^2(i\pi x/l)\, \mathrm{d}x + \sum_{i=1}^{N}\sum_{j=1}^{N} (a_{t\alpha i} - a_{\alpha i})(a_{t\alpha j} - a_{\alpha j}) \int_0^l \sin(i\pi x/l) \sin(j\pi x/l)\, \mathrm{d}x, \qquad i \neq j. \tag{108}$$

Performing the integration as indicated in equation (108) and realizing that $\int_0^l \sin^2(i\pi x/l)\, \mathrm{d}x = l/2$ and $\int_0^l \sin(i\pi x/l) \sin(j\pi x/l)\, \mathrm{d}x = 0$, $i \neq j$, one obtains

$$\frac{l}{2} \sum_{i=1}^{N} [(a_{t\alpha i} - a_{\alpha i})^2]. \tag{109}$$

Thus the criterion of equation (28) can be written in terms of the eigenfrequencies $\xi_{\alpha i}$ and the coefficients $a_{\alpha i}$ and $a_{t\alpha i}$ of the Fourier expansions:

$$\min_{\mathbf{x}_2} \sum_{\alpha=1}^{M} \left[(\xi_{t\alpha} - \xi_\alpha)^2) + \sum_{i=1}^{N} (a_{t\alpha i} - a_{\alpha i})^2 \right], \tag{110}$$

where the variable vector $\mathbf{x}_2 = \{cr, xc, \xi_\alpha, a_{\alpha i}\}$.

Now, substituting equations (106) and (107) into the constraints, equations (29) and (30), and then integrating with respect to x, the latter equations can be written in matrix form as

$$\tilde{a}_\alpha^T [K_0] \tilde{a}_\alpha - \xi_\alpha \tilde{a}_\alpha^T \tilde{a}_\alpha = 0, \qquad \tilde{a}_\alpha^T \tilde{a}_\alpha - \delta_{\alpha\beta} = 0, \qquad 0 \leqslant cr \leqslant 1, \qquad 0 \leqslant xc \leqslant 1, \tag{111-114}$$

where matrix $[K_0]$ is defined as

$$[K_0] = i^2 j^2 \int_0^l Q(x) \sin(i\pi x/l) \sin(j\pi x/l)\, \mathrm{d}x, \qquad i, j = 1, \ldots, N, \tag{115}$$

and where $\tilde{a} = (a_1, a_2, \ldots, a_N)^T$.

3.2. FORMULATION OF THE MIN MAX PROBLEM FOR THE NUMERICAL METHOD

By following an approach similar to that of the previous subsection, the min-max problem formulation for the numerical method also can be stated easily in a form that is appropriate for computational implementation. The results for the two cases of discrete and continuous expression for the test data are as follows.

3.2.1. *Discrete testing deflection data*

$$\min_{\mathbf{x}_1} (\Psi), \tag{116}$$

subject to

$$\left[\sum_{\alpha=1}^{M}[(\xi_{t\alpha}-\xi_\alpha)^2+\sum_{i=1}^{T}(w_{t\alpha}(x_{tm})-w_\alpha(x_{tm}))^2\right]-\Psi\leqslant 0, \tag{117}$$

$$\left[\alpha^4 Q\sum_{m=1}^{T}(w_\alpha(x_{tm}))^2-\xi_\alpha\sum_{m=1}^{T}(w_\alpha(x_{tm}))^2\right]\Delta x_{tm}-\Upsilon_\alpha=0, \tag{118}$$

$$\sum_{m=2}^{T-1}(w_\alpha(x_{tm})w_\beta(x_{tm}))\Delta x_{tm}-\eta_{\alpha\beta}=0, \tag{119}$$

$$0\leqslant cr\leqslant 1, \qquad 0\leqslant xc\leqslant 1. \tag{120, 121}$$

3.2.2. *Continuous testing deflection data*

$$\min_{x_2}(\Psi), \tag{122}$$

subject to

$$\left[\sum_{\alpha=1}^{M}\left[(\xi_{t\alpha}-\xi_\alpha)^2)+\sum_{i=1}^{N}(a_{tai}-a_{\alpha i})^2\right]-\Psi\right]\leqslant 0, \tag{123}$$

$$\tilde{a}_\alpha^T[K_0]\tilde{a}_\alpha-\xi_\alpha\tilde{a}_\alpha^T\tilde{a}_\alpha=0, \qquad \tilde{a}_\alpha^T\tilde{a}_\alpha-\delta_{\alpha\beta}=0, \qquad 0\leqslant cr\leqslant 1, \qquad 0\leqslant xc\leqslant 1, \tag{124–127}$$

where $\alpha, \beta=1,\ldots,M$.

4. NUMERICAL EXAMPLES

The numerical optimization technique set forth in this study for vibrating cracked beam identification problems is accomplished using the VMCON optimization package program (this implements a sequential quadratic programming method). The VMCON program uses Powell's algorithm, which is an iterative scheme designed to converge to a point that satisfies the necessary conditions. Additional information regarding to VMCON is available in reference [32].

Unless otherwise stated, the damage properties (cr and xc) of the simply supported cracked beams are identified by direct solution of the optimalization problems described in the previous section. The sensitivity to chosen values for the initial crack position xc are discussed later in this section.

The cracked beam model to which the identification procedure is applied is shown in Figure 1. It is a simply supported beam of length l equal to 18·11 of its thickness $2d$, with uniform rectangular cross-section area A, and a pair of symmetric cracks of $cr=0{\cdot}5$ located at mid-span ($xc=0{\cdot}5$).

4.1. EXAMPLES WITH POSITION OF THE CRACK (DAMAGE) SPECIFIED

Consider the first example for crack identification, the simply supported cracked beam, for which the crack position xc is known. In other words, only the crack ratio cr is to be identified; therefore, the variables in this problem are cr, the ξs, and mode shapes $w_\alpha(x)$ ($\mathbf{x}_1=\{cr, \xi_\alpha, w_\alpha(x_{tm})\}$, $\mathbf{x}_2=\{cr, \xi_\alpha, a_{\alpha i}\}$). This simplified example problem with the crack position specified ($xc=0{\cdot}5$) is presented to demonstrate the concept of the crack identification procedure described in section 2.

TABLE 1

Numerical results based on the mean square problem statement of equations (99–103) with the crack (damage) specified ($xc = 0{\cdot}5$)

Test data: $\xi_1^* = 0{\cdot}84703$, $\xi_3^* = 70{\cdot}1348$, $cr^* = 0{\cdot}5$

Initial data			Final data		
ξ_1	ξ_3	cr	ξ_1	ξ_3	cr
1·0	81·0	0·0	0·84684	70·1348	0·50033
0·98841	80·0769	0·1	0·84697	70·1346	0·50019
0·97217	78·8135	0·2	0·84704	70·1347	0·49998
0·94815	77·0062	0·3	0·84701	70·1348	0·50007
0·91032	74·3024	0·4	0·84694	70·1347	0·50024
0·73638	63·7848	0·6	0·84705	70·1348	0·49962
0·54574	55·0511	0·7	0·84703	70·1348	0·50034
0·27233	45·9316	0·8	0·84700	70·1347	0·50009

4.1.1. *Discrete testing deflection data*

In this example, it is assumed that the dynamic measurements are collected at nine test positions ($T = 9$) equally spaced over the span. The first and last test stations are located at the left and right supported end, respectively. Hence, the length of each test span Δx_{tm}, $m = 1, \ldots, T-1$, is determined to be $36{\cdot}22d/(T-1)$. In structural dynamic testing, ordinarily only a relatively small subset of the theoretically available eigenvalues and eigenvectors can be measured accurately; i.e., realistic information on higher modes is difficult to obtain from the measurements at a limited set of test stations. Only information

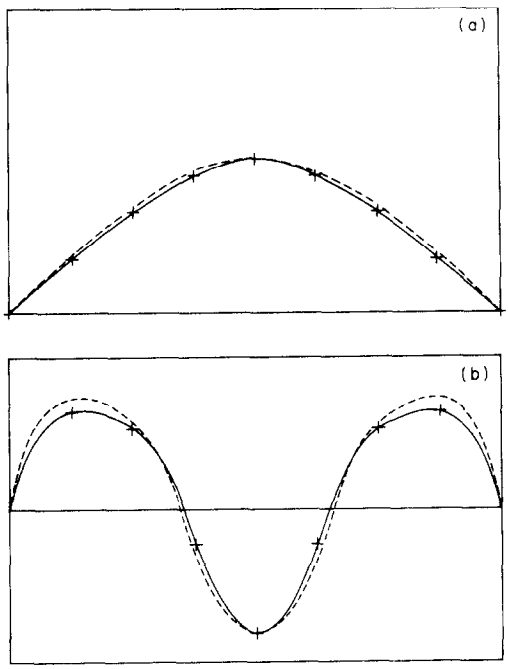

Figure 2. Comparison between the initial, final and test mode shapes in (a) the first mode and (b) the third mode. The crack identification process is based on the mean square formulation with a specified crack position xc and nine test stations. The beam is simply supported with symmetric cracks at mid-span, for $cr = 1/2$. The initial data is selected at $cr = 0{\cdot}0$. Mode shapes: +, test; - - -, initial; ——, final.

from the first three modes is to be used as test data in the present identification process. Furthermore, according to the observations in Shen and Pierre [10], the even modes of a simply supported beam are not sensitive to a mid-span crack; therefore, in effect only first and third mode ($\alpha = 1, 3$) information is used to represent crack damage.

TABLE 2

Numerical results based on the min–max problem statement of equations (116–121) with the crack (damage) specified ($xc = 0{\cdot}5$)

Test data: $\xi_1^* = 0{\cdot}84703$, $\xi_3^* = 70{\cdot}1348$, $cr^* = 0{\cdot}5$

Initial data			Final data		
ξ_1	ξ_3	cr	ξ_1	ξ_3	cr
1·0	81·0	0·0	0·84823	70·1382	0·49423
0·98841	80·0769	0·1	0·84905	70·1354	0·49152
0·97217	78·8135	0·2	0·84821	70·1355	0·49482
0·94815	77·0062	0·3	0·84714	70·1378	0·49943
0·91032	74·3024	0·4	0·84865	70·1371	0·49265
0·73638	63·7848	0·6	0·84715	70·1369	0·49919
0·54574	55·0511	0·7	0·84637	70·1354	0·50167
0·27233	45·9316	0·8	0·84708	70·1345	0·49959

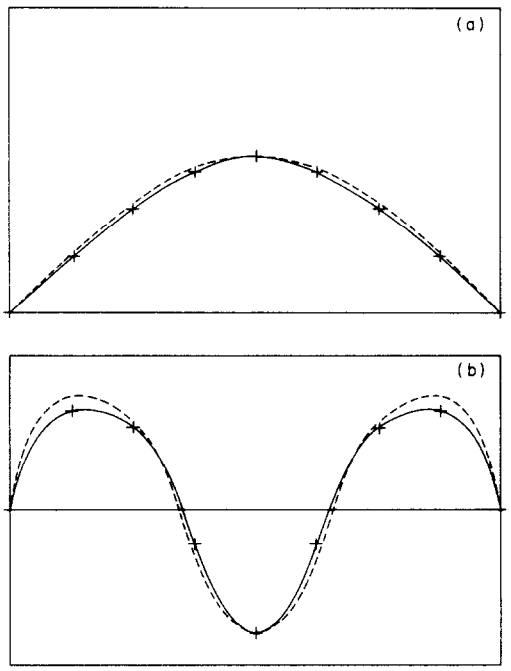

Figure 3. Comparison between the initial, final and test mode shapes (a) in the first mode and (b) the third mode. The crack identification process is based on the min–max formulation with a specified crack position xc and nine test stations. The beam is simply supported with symmetric cracks at mid-span, for $cr = 1/2$. The initial data is selected at $cr = 0{\cdot}0$. Mode shapes: +, test; – –, initial; ——, final.

Mean square criterion. Once again, the crack identification problem of equations (99–103) presented in section 3.1 is solved here with a specified value $xc = 0{\cdot}5$. For given initial values of $\mathbf{x}$, this optimization problem is solved to minimize the criterion F. The results of

the cases with various initial conditions are shown in Table 1. In order to clearly compare the results, only the first three variables, ξ_1, ξ_3 and cr, of variable vector $\mathbf{x}_1$ are listed in Table 1. However, a more detailed listing of the corresponding initial, final and testing variable vectors $\mathbf{x}_1$ is provided in Appendix A. The values of criterion and constraint are also shown in Appendix A.

In Table 1, the top row denotes the assumed crack ratio and corresponding first and third eigenfrequencies. The symbol * denotes the expected optimal solution through the identification process. The first two column entries, ξ_1, and ξ_3, indicate the fundamental and the third frequencies corresponding to the initial crack ratio cr which is given in the next column. The last three columns give the final values corresponding to previous entry values. These final values are obtained at the stage at which computation is terminated when the further optimal search obtains improvements for criterion F less than the specified tolerance (10E−5 was adopted in the present study). Recall that for an uncracked beam cr is identically zero. Therefore, in this example, it is decided to start with the case of the initial value $cr=0{\cdot}0$ and for each case thereafter the cr value is increased by 0·1.

TABLE 3

Numerical results based on the mean square problem statement of equations (111–114) with the crack (damage) specified ($xc=0{\cdot}5$)

Test data: $\xi_1^*=0{\cdot}88884$, $\xi_3^*=72{\cdot}8794$, $cr^*=0{\cdot}5$

Initial data			Final data		
ξ_1	ξ_3	cr	ξ_1	ξ_3	cr
1·0	81·0	0·0	0·88883	72·8791	0·50001
0·98907	80·1290	0·1	0·88877	72·8755	0·50012
0·97527	79·0542	0·2	0·88887	72·8736	0·50017
0·95671	77·6497	0·3	0·88878	72·8756	0·50011
0·93001	75·7007	0·4	0·88880	72·8773	0·50006
0·82063	68·6035	0·6	0·88889	72·8835	0·49988
0·69955	62·0801	0·7	0·88875	72·8740	0·50016
0·48039	52·9197	0·8	0·88874	72·8730	0·50019

TABLE 4

Numerical results based on the min–max problem statement of equations (122–127) with the crack (damage) specified ($xc=0{\cdot}5$)

Test data: $\xi_1^*=0{\cdot}88884$, $\xi_3^*=72{\cdot}8794$, $cr^*=0.5$

Initial data			Final data		
ξ_1	ξ_3	cr	ξ_1	ξ_3	cr
1·0	81·0	0·0	0·88919	72·9031	0·49930
0·98907	80·1290	0·1	0·88873	72·8726	0·50020
0·97526	79·0542	0·2	0·88888	72·8779	0·50004
0·95671	77·6497	0·3	0·88881	72·8778	0·50005
0·93001	75·7067	0·4	0·88881	72·8779	0·50004
0·82063	68·6034	0·6	0·88882	72·8783	0·50003
0·69955	62·0801	0·7	0·88881	72·8775	0·50005
0·48039	52·9197	0·8	0·88897	72·8882	0·49974

From the results presented in the first case of Table 1 and the Appendix, one sees that the parameters ξ_1, ξ_3 and cr were identified to be 0·84684, 70·1348 and 0·50033 from 1·0, 81·0 and 0·0, respectively. The mean square criteria F was cut down from 118·13502 to 0·42440E−5. The maximum error is less than 0·5% of the test data for these parameters.

The results are also quite impressive, as noted in Appendix A, which contains initial, final and testing mode shapes. In order to observe the global variance clearly, these modes are plotted in Figure 2. Three curves appear on each plot: the initial mode shape, the final mode shape, and the mode shape from the test response. The final mode shape on these plots agrees well with the test mode shape. This is expected and verifies the accuracy observed from the results in Table 1. It can be clearly seen that accuracy of the mode shapes will worsen if higher mode results are to be predicted. Improvement can be obtained by an appropriate adjustment of the location of these test stations. However, a sensitivity analysis of the test stations with respect to the accuracy of the dynamic measurements is required. This is not considered further in the present study.

TABLE 5

Numerical results based on the mean square problem statement of equations (99–103); *the position of the damage xc is a variable*

Test data: $\xi_1^* = 0{\cdot}84703$, $\xi_3^* = 70{\cdot}1348$, $cr^* = 0{\cdot}5$, $xc^* = 0{\cdot}5$

	Initial data				Final data			
T	ξ_1	ξ_3	cr	xc	ξ_1	ξ_3	cr	xc
9	0·91806	78·5161	0·4	0·4	0·69639	70·1359	0·99789	0·36289
9	0·91371	76·6365	0·4	0·43	0·70007	70·1362	0·99440	0·39620
9	0·91158	75·1335	0·4	0·46	0·84610	70·1347	0·91029	0·53775
9	0·91056	74·7464	0·4	0·47	0·84711	70·1347	0·67125	0·49033
9	0·91063	74·5157	0·4	0·48	0·84704	70·1348	0·50554	0·49972
9	0·73472	63·8062	0·6	0·51	0·84704	70·1348	0·60027	0·50526
9	0·73711	64·2643	0·6	0·52	0·84704	70·1348	0·60083	0·50531
9	0·73617	64·7619	0·6	0·53	0·84704	70·1348	0·60141	0·50534
9	0·73929	65·6727	0·6	0·54	0·84705	70·1348	0·60255	0·49459
9	0·73909	66·6112	0·6	0·55	0·84702	70·1348	0·99721	0·24709
9	0·75452	74·0109	0·6	0·6	0·70040	70·1363	0·99079	0·59307
45	0·97475	80·2193	0·2	0·4	0·90130	70·1347	0·94855	0·94404
45	0·91806	78·5161	0·4	0·4	0·84420	70·1345	0·53053	0·51586
45	0·91531	77·2676	0·4	0·42	0·84686	70·1347	0·50838	0·50198
45	0·96219	78·5819	0·25	0·45	0·84643	70·1348	0·51729	0·49389
45	0·75452	74·0109	0·6	0·6	0·84645	70·1348	0·51723	0·50609
45	0·64083	77·7173	0·7	0·7	0·89079	70·1347	0·58895	0·81817

In Table 1, rows 5–11 present the results for cases with initial $cr = 0{\cdot}1$ to $0{\cdot}8$. The corresponding final point values listed in columns 4–6 show that these cases exhibit, as expected, similar solution characteristics and accuracy. This provides a physical understanding of the geometry of the solution set: for the inverse cracked beam problem with specified crack position, the mean square criterion of equation (99) is a convex function and it is bounded by the constraints of equations (100–103). Hence, one may conclude that the convergence of the present optimization problem is obtained independent of the initial data chosen. In other words, as long as the initial data is selected within the problem's feasible domain, an accurate and unique solution through the identification process is expected.

Clearly the prediction of the mode 3 shape shown in Figure 2 fails to reproduce the expected sine curve. This is because the third mode shape was plotted based on the deflections of the mode shape measured at only nine test stations. While this reflects a limitation on how well mode shapes are portrayed, the quality of the final result for the identification problem is unaffected.

Min–max problem. The present example identification problem was also demonstrated using the min–max formulation. To validate the observations from the previous results,

the same cases treated above were solved based on the min–max formulation, and the first free variables, ξ_1, ξ_3 and cr of vector $\mathbf{x}_1$ are listed in Table 2. As shown in Table 2, the agreement of the final data and the test data is similar to those in Table 1. The maximum error observed at the final iteration of vector $\mathbf{x}_1$ is approximately 0·7% of the test data. Figure 3 shown the initial, final, and test mode shapes of the first case in Table 2. Notice that the excellent agreement between the final and test mode shapes shows a similar solution convergence as was seen in Figure 2. Thus, one can conclude that in the present cracked beam problem with a specified crack position, the min–max formulation provides an accurate and unique solution of equal quality to that of the mean square error criteria problem illustrated via previous example.

4.1.2. *Continuous testing deflection data*

In this example, it is assumed that the dynamic measurements information is available in the form of continuous function expressions for mode shapes. The identification procedure uses first and third mode information which are approximated using a 25-term Fourier series.

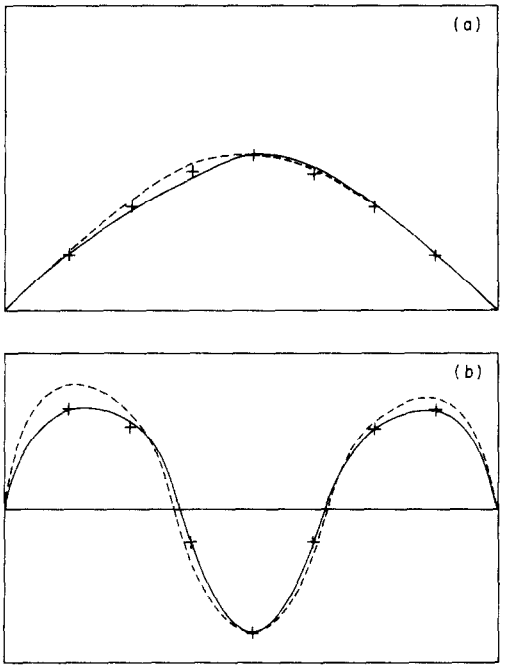

Figure 4. Comparison between the initial, final and test mode shapes in (a) the first mode and (b) the third mode. The crack identification process is based on the mean square formulation, in which both crack position xc and crack ratio cr are unknown, and nine test stations. The beam is simply supported with symmetric cracks at mid-span, for $cr = 1/2$. The initial data is selected at $cr = 0{\cdot}4$, $xc = 0{\cdot}4$. Mode shapes: +, test; - - -, initial; ——, final.

The identification procedure uses first and third mode information which should be approximated, as it was suggested in reference [10], using an at least 150-term Fourier series. However, in the present case, in order to avoid huge computational efforts, only 25 terms are used. As a result, the test data ξ_1^* and ξ_3^* provided in Tables 3 and 4 have higher values than those shown in Tables 1 and 2.

Mean square criterion. The crack identification problem of equations (110–114), presented in section 3.1, is solved with the value of the variable xc specified. For a given initial value

of $\mathbf{x}_2$, this optimization problem is solved to minimize the criterion F. The results of the cases with various starting point values are shown in Table 1. In order to provide a clear comparison of the results, only the partial listing comprised of the first three variables, ξ_1, ξ_3 and cr, of variable vector $\mathbf{x}_2$ are listed in Table 3.

As shown in Table 3, good agreement between the final modelled values and the given test data is obtained, similar in quality to the earlier results given in Tables 1 and 2. However, since the identification process is required to generate the 25×25 stiffness matrix at each search step, the computational effort for the present example is much greater than that for the discrete deflection data. In any case, the effectiveness (robustness) of the model for this identification problem is substantiated, based on its successful performance over such a broad range of starting values.

Min–max problem. The present example identification problem was also treated according to the min–max formulation. To validate the observations from the previous results, the same initial positions as those represented in Table 3 were tested using the min–max formulation. As shown in Table 4, the agreement between the final identification results and the given test data is similar in quality to what was obtained in the earlier example.

In summary, for the present cracked beam problem with crack positions specified, the min–max formulation provided the basis for an identification solution as accurate as the mean square criterion form of the problem.

4.2. SIMULTANEOUS IDENTIFICATION OF CRACK POSITION AND DEPTH

The second numerical example deals with the crack identification of a simply supported cracked beam with unknown crack ratio and with crack position unknown. In this treatment, the variables in the optimization problem are cr, xc, ξs, and mode shapes $w_\alpha(x)$

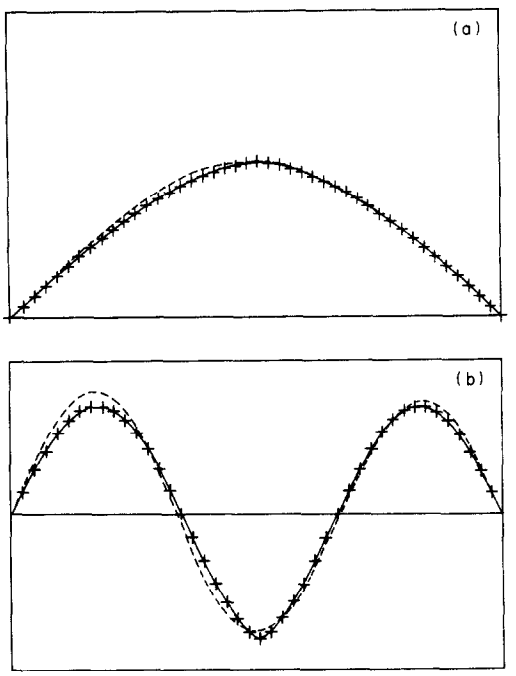

Figure 5. Comparison between the initial, final and test mode shapes in (a) the first mode and (b) the third mode. The crack identification process is based on the mean square formulation, in which both crack position xc and crack ratio cr are unknown, and 45 test stations. The beam is simply supported with symmetric cracks at mid-span, for $cr = 1/2$. The initial data is selected at $cr = 0{\cdot}4$, $xc = 0{\cdot}4$. Mode shapes: +, test; - - -, initial; ——, final.

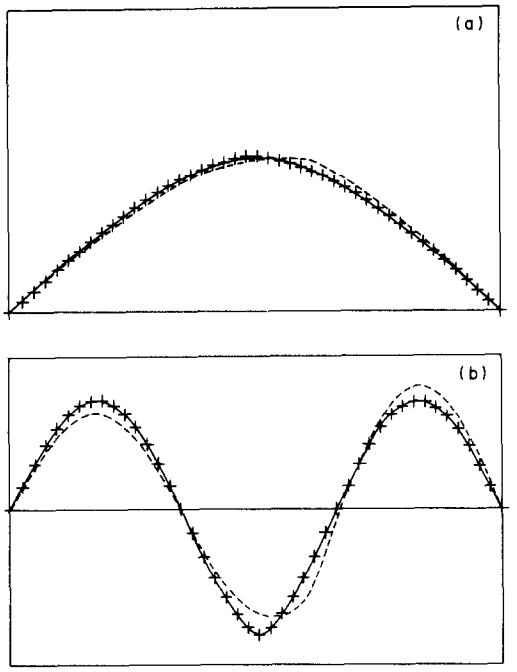

Figure 6. Comparison between the initial, final and test mode shapes in (a) the first mode and (b) the third mode. The crack identification process is based on the mean square formulation, in which both crack position xc and crack ratio cr are unknown, and 45 test stations. The beam is simply supported with symmetric cracks at mid-span, for $cr=1/2$. The initial data is selected at $cr=0{\cdot}6$, $xc=0{\cdot}6$. Mode shapes: +. test; - - , initial; ——, final.

($\mathbf{x}_1=\{cr, xc, \xi_a, w_a(x_{tm})\}$). Due to the limitations of the VMCON program, examples concerning the testing mode shapes w_t provided in the form of continuous functions are not shown in this subsection.

4.2.1. *Discrete testing deflection data*

Mean square criterion. The formulation of the crack identification problem of equations (99–103) presented in section 3.1 is tested here. In the first few cases, the simulated dynamic test measurements are assumed to be collected at nine equally spaced test stations ($T=9$). The first and last test positions are located at the left and right supported ends, respectively. This example will be solved for a second time using an increased number of test stations, to provide information on the sensitivity of the procedure to the amount of test data.

In Table 5, the top row denotes the assumed crack ratio, the crack position and the corresponding first and third eigenfrequencies. The symbol * denotes the expected optimal solution through the identification process. The first column entry T denotes the number of test stations used to collect dynamic measurements. The second and third column entries, ξ_1, ξ_3, indicate the fundamental and the third frequencies corresponding to the initial crack ratio cr and crack position xc, which are given in the next two columns. The last four columns provide the final values corresponding to the previous entry values. These final values are obtained at the stage at which the computation is terminated when the optimal search obtains step-wise improvements of F less than a specified tolerance (10E − 5 in the present study).

TABLE 6

Numerical results based on the min–max problem statement of equations (116–121); *the position of the damage xc is a variable*

Test data: $\xi_1^* = 0{\cdot}84703$, $\xi_3^* = 70{\cdot}1348$, $cr^* = 0{\cdot}5$, $xc^* = 0{\cdot}5$

	Initial data				Final data			
T	ξ_1	ξ_3	cr	xc	ξ_1	ξ_3	cr	xc
9	0·91806	78·5161	0·4	0·4	0·84702	70·1348	0·99721	0·24709
9	0·91371	76·6365	0·4	0·43	0·84697	70·1348	0·86044	0·47182
9	0·91158	75·1335	0·4	0·46	1·03879	70·1365	0·75507	0·87498
9	0·91032	74·3024	0·4	0·47	0·84697	70·1348	0·85985	0·52812
9	0·91063	74·5157	0·4	0·48	0·84844	70·1328	0·49455	0·49998
9	0·73472	63·8062	0·6	0·51	0·84661	70·1102	0·60027	0·50519
9	0·73711	64·2643	0·6	0·52	0·84672	70·1119	0·60084	0·50523
9	0·73617	64·7619	0·6	0·53	0·84664	70·1139	0·60247	0·49471
9	0·73929	65·6727	0·6	0·54	0·90724	70·1524	0·83845	0·37496
9	0·73909	66·6112	0·6	0·55	0·84621	70·1350	0·71880	0·48705
9	0·75452	74·0109	0·6	0·6	0·73638	63·7848	0·99875	0·64976
45	0·99017	79·0380	0·2	0·2	0·84693	70·1347	0·79372	0·24988
45	0·91806	78·5161	0·4	0·4	0·84654	70·1346	0·51636	0·49454
45	0·96219	78·5818	0·25	0·45	0·84723	70·1388	0·50602	0·50188
45	0·75452	74·0109	0·6	0·6	0·84685	70·1348	0·51687	0·50588
45	0·77533	80·2259	0·6	0·65	0·83005	70·1492	0·60871	0·54193
45	0·64083	77·7173	0·7	0·7	0·84824	70·1366	0·78866	0·75124

It is shown in Table 5 that cases with $T=9$ have the final values of ξ close to ξ^*, but almost all of these cases have unacceptable final estimates of xc and cr. For instance, if the initial position is selected as $xc=0{\cdot}4$ and $cr=0{\cdot}4$, the values of xc and cr at the final iteration are 0·99789 and 0·36289, which differ approximately 98% and 28% from the given test data. Evidently, the configuration with $xc=0{\cdot}99789$ and $cr=0{\cdot}36289$ is able to provide another minimum value of the criterion (besides the one associated with the expected result). This cracked beam configuration is shown in the solid curve of Figure 4. The mismatch between final and test mode shapes can be clearly seen. This observation confirmed the unacceptable error previously obtained in the comparison of xc and cr between the final and test data. Except for the case with initial $cr=0{\cdot}4$ and $xc=0{\cdot}48$, which provides less than 1% estimation error, the rest of the cases in Table 5 with nine test stations are also found to have similarly large estimation errors. Therefore a dependable solution in crack identification is almost impossible to achieve on the basis of the nine test stations simulated measurement information using first and third mode response. This confirmed the observations by Shen and Pierre [10, 11], i.e., for a cracked beam with an unknown crack position, a unique solution is not to be expected.

However, by comparing the third mode shape in Figures 2(b), 3(b) and 4(b) with the mode shape in Figure 11(c) of reference [10], it can be seen that an accurate third mode shape cannot be approximated on the basis of the displacements collected from nine test stations only. This implies that the accuracy of the above computational identification might be improved if the third mode is approximated well. Therefore, cases with more test stations should be examined, since they would clearly allow better mode shape approximations. The largest number of test stations which can be accommodated in the identification procedure is 45, due to the limitations of the optimization program package. Once again, the test measurement points are equally spaced, and the first and last stations are located at the left and right supported ends, respectively. The VMCON problem formulation

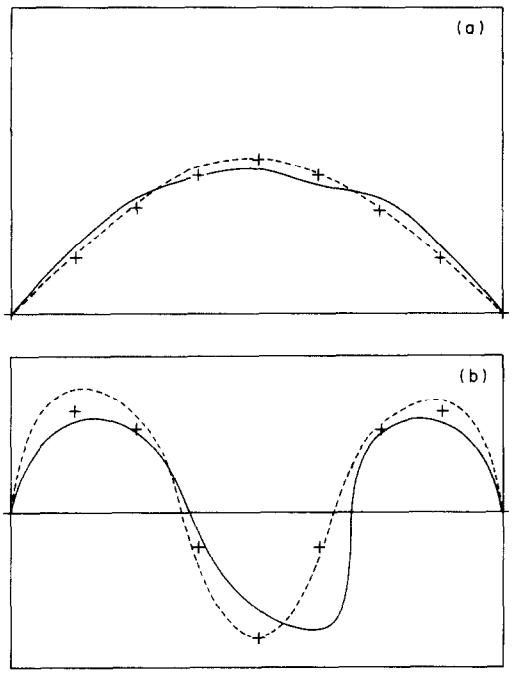

Figure 7. Comparison between the initial, final and test mode shapes in (a) the first mode and (b) the third mode. The crack identification process is based on the min–max formulation, in which both crack position xc and crack ratio cr are unknown, and nine test stations. The beam is simply supported with symmetric cracks at mid-span, for $cr=1/2$. The initial data is selected at $cr=0{\cdot}4$, $xc=0{\cdot}4$. Mode shapes: +, test; - - -, initial; ——, final.

is identical to the case of $T=9$; however, the variable vector $\mathbf{x}$ is expanded from 22 components to 94.

Rows 12–17 of Table 5 summarize the results through the minimization process. As in the previous cases, the final values of frequency ξ are observed to be close to test values ξ^*. Acceptable final solution values for xc and cr are shown in the results of the cases in which initial xc and cr are selected within the range from $xc=0{\cdot}4$, $cr=0{\cdot}4$ to $xc=0{\cdot}6$, $cr=0{\cdot}6$. On the other hand, within this range, good agreement is also shown in mode shapes. In Figures 5 and 6 are displayed the initial, final and test mode shapes for cases with the initial $xc=0{\cdot}4$, $cr=0{\cdot}4$ and $xc=0{\cdot}6$, $cr=0{\cdot}6$. Excellent agreement is observed between the final and test mode shapes. Moreover, by comparing the final data curve in Figures 5 and 6 with the mode shape in Figure 11(c) of reference [10], a more accurate third mode is approximated. This indicates that more accurate information on mode shapes is required to obtain a satisfactory solution from the identification process in the case where both crack position and crack depth are unknown.

Questions arise concerning the conditions under which the identification procedure can provide an unique solution. As discussed by Shen and Pierre [10, 11] and concluded in the studies of Gladwell *et al.* [28], if all the mode information is used in the identification procedure, then the system's properties can be identified uniquely. However, for practical reasons, in structural dynamic testing only a small subset of the eigenvalues and eigenvectors can be represented in the measurement data. Furthermore, even if substantially more modal information would be available, the minimization search may be prohibitive for such the large-dimensional domain that would result. These comments are intended to point out certain limitations inherent in the identification procedures. These considerations

will be addressed again in the authors' next study, which describes sufficient conditions for unique identification from the dynamic measurements of a multi-degree-of-freedom vibrating spring–mass system.

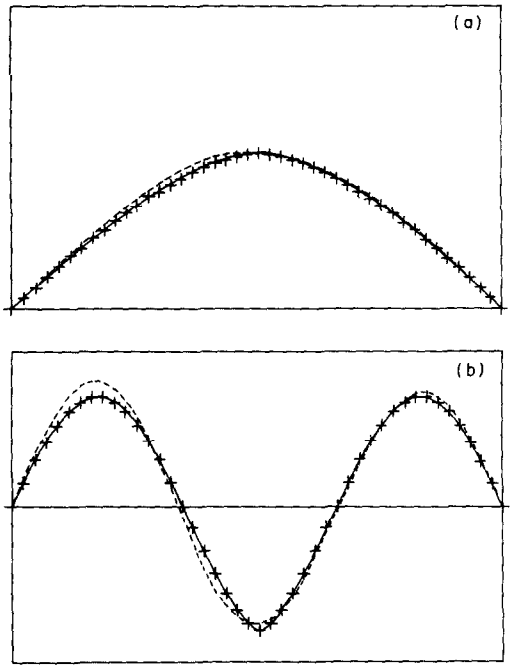

Figure 8. Comparison between the initial, final and test mode shapes in (a) the first mode and (b) the third mode. The crack identification process is based on the min–max formulation, in which both crack position xc and crack ratio cr are unknown, and 45 test stations. The beam is simply supported with symmetric cracks at mid-span, for $cr = 1/2$. The initial data is selected at $cr = 0{\cdot}4$, $xc = 0{\cdot}4$. Mode shapes: +, test; - - -, initial; ——, final.

Min–max treatment: both positions and crack depth unknown. To validate observations from the previous results, the case shown in Table 5 were solved again using the min–max formulation. The first four variables, ξ_1, ξ_3, cr and xc, of vector $\mathbf{x}_I$ are listed in Table 6 and the initial, final and test mode shapes for the cases with initial $xc = 0{\cdot}4$, $cr = 0{\cdot}4$, with $T = 9$, and 45, and $xc = 0{\cdot}6$, $cr = 0{\cdot}6$, with $T = 45$, are displayed in Figures 7–9, respectively.

This demonstrates the similarity of the solution characteristics between the present min–max formulation and the mean square criterion formulation, much the same as illustrated for the previous example.

5. CONCLUSIONS

A general method for crack identification of a simple beam with one pair of symmetric cracks is presented. The method may be useful as a component of an on-line non-intrusive damage detection technique for vibrating structures. A variational formulation is expressed as a direct minimization problem statement using the criteria of the mean square difference of natural frequencies and mode shapes between test measurements and corresponding model values. This problem is formulated a second time as a scalar form min–max problem with an additional inequality constraint. The necessary conditions are obtained for each of these formulations. The crack identification problem is reduced to finding the cracked

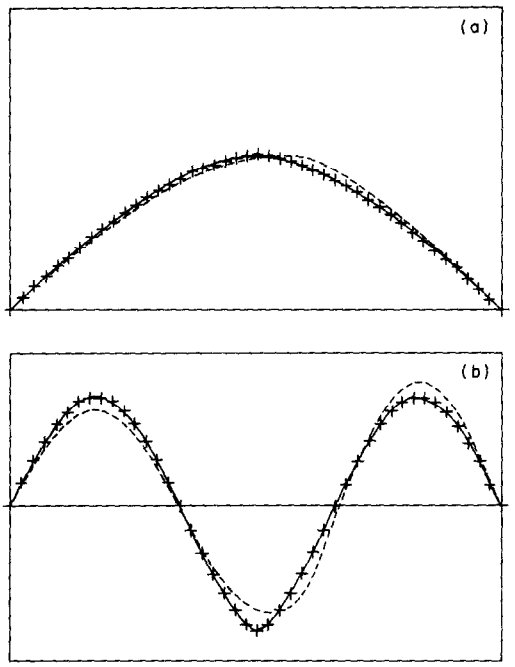

Figure 9. Comparison between the initial, final and test mode shapes in (a) the first mode and (b) the third mode. The crack identification process is based on the min-max formulation, in which both crack position xc and crack ratio cr are unknown, and 45 test stations. The beam is simply supported with symmetric cracks at mid-span, for $cr=1/2$. The initial data is selected at $cr=0{\cdot}6$, $xc=0{\cdot}6$. Mode shapes: +, test; - - -, initial; ——, final.

beam's damage parameters that will satisfy appropriate constraints and minimize the means square difference, or the appropriate criterion in the min-max treatment.

The uniqueness and reliability of the identification process is confirmed by solving several crack identification examples with specified crack positions. Without knowing the damaged location, a restricted region in initial data space has been found for which there will be a realistic and convergent solution from the identification process. This region is small, and can be expanded if modal variables are well approximated and initial data corresponding to higher modes of the beam are included in the process.

REFERENCES

1. G. R. IRWIN 1980 *Structural Mechanics* (P. C. Goodier and N. J. Hoff, editors), 557. Oxford: Pergamon Press. See the fracture mechanics section.
2. P. C. PARIS and G. C. SIH 1965 *Facture Toughness and its Applications*, *ASME STP*-**381**, 30. Stress analysis of cracks.
3. I. W. MAYES and W. G. R. DAVIES 1976 *Conference on Vibrations in Rotating Machinery* (*IME Conference*), C168/76, 53–64. The vibrational behaviour of a rotating shaft system containing a transverse crack.
4. T. A. HENRY and B. E. OKAH-AVAE 1976 *Conference on Vibrations in Rotating Machinery* (*IME Conference*), C162/76, 15–19. Vibration in cracked shaft.
5. P. CAWLEY and R. D. ADAMS 1979 *Journal of Strain Analysis* **14**, 49–57. The location of defects in structures from measurements of natural frequencies.

6. A. D. DIMAROGONAS and C. A. PAPADOPOULOS 1983 *Journal of Sound and Vibration* **91**, 583–593. Vibration of cracked shafts in bending.
7. P. GUDMUNDSON 1983 *Journal of the Mechanics and Physics of Solids* **31**, 329–345. The dynamic behaviour of slender structures with cross-sectional cracks.
8. C. A. PAPADOPOULOS and A. D. DIMAROGONAS 1987 *Ingenieur-Archiv* **57**, 257–266. Coupling of bending and torsional vibration of a cracked Timoshenko shaft.
9. S. CHRISTIDES and A. D. S. BARR 1984 *International Journal of the Mechanical Sciences* **26**, 639–648. One-dimensional theory of cracked Bernoulli–Euler beams.
10. M. H. SHEN and C. PIERRE 1990 *Journal of Sound and Vibration* **138**, 115–134. Natural modes of Bernoulli–Euler beams with symmetric cracks.
11. M. H. SHEN and C. PIERRE 1990 *AIAA/ASME/ASCE/ASH 31th Structures, Structural Dynamics and Materials Conference Proceedings* **4**, 2079–2093. Natural modes of Bernoulli–Euler beams with a single edge crack.
12. G. BORG 1946 *Acta Mathematica* **78**, 1–96. Eine Umkehrung der Sturm–Liouvilleschen Eigenwertaufgabe.
13. I. M. GEL'FAND and B. M. LEVITAN 1951 *American Mathematical Society Translations* **1**, Series 2, 253–304. On the determination of a differential equation from its spectral function.
14. I. M. GEL'FAND and B. M. LEVITAN 1953 (in Russian) *Doklady Akademiia Nauk SSSR* **88**, 337–357. On a simple identify for the characteristic values of a differential operator of the second order.
15. G. E. BACKUS and J. F. GILBERT 1967 *Geophysical Journal of the Royal Astronomical Society* **13**, 247–276. Numerical applications of a formalism for geophysical inverse problems.
16. R. G. NEWTON 1970 *SIAM Review* **12**, 346–356. Inverse problems in physics.
17. V. BARCILON 1974 *Journal of Mathematical Physics* **15**, 429–436. Iterative solution of the inverse Sturm–Liouville equation.
18. V. BARCILON 1974 *Geophysical Journal of the Royal Astronomical Society* **38**, 287–298. On the uniqueness of inverse eigenvalue problems.
19. V. BARCILON 1974 *Geophysical Journal of the Royal Astronomical Society* **39**, 143–154. On the solution of inverse eigenvalue problems of high orders.
20. V. BARCILON 1976 *Zeitschrift fuer Angewandte Mathematik und Physik* **27**, 346–358. Inverse problem for a vibrating beam.
21. J. R. MCLAUGHLIN 1976 *SIAM Journal of Mathematical Analysis* **7**, 646–661. An inverse problem of order four.
22. J. R. MCLAUGHLIN 1984 *Inverse Problems of Acoustic and Elastic Waves* (F. Santosa, W. W. Symes, Y. H. Pao and C. Holland, editors) 341–347. SIAM. On constructing solutions to an inverse Euler–Bernoulli beam problem.
23. J. R. MCLAUGHLIN 1986 *SIAM Review* **28**, 53–72. Analytical methods for recovering coefficients in Sturm–Liouville equations.
24. V. BARCILON 1982 *Philosophical Transactions of the Royal Society of London* **304**, Series A, 211–252. Inverse problems for the vibrating beam in the free–clamped configuration.
25. G. M. L. GLADWELL 1984 *Proceedings of the Royal Society of London* **393**, Series A, 277–295. The inverse problem for the vibrating beam.
26. G. M. L. GLADWELL 1985 *Proceedings of the Royal Society of London* **401**, Series A, 299–315. Qualitative properties of vibrating beam.
27. G. M. L. GLADWELL 1986 *Proceedings of the Royal Society of London* **407**, Series A, 199–218. The inverse problem for the Euler–Bernoulli beam.
28. G. M. L. GLADWELL, A. H. ENGLAND and D. WANG 1987 *Journal of Sound and Vibration* **119**, 81–94. Examples of reconstruction of an Euler–Bernoulli beam from spectral data.
29. J. R. MCLAUGHLIN 1981 *Proceedings of the International Conference on Spectral Theory of Differential Operators, University of Alabama, Birmingham.* Fourth order inverse eigenvalue problems.
30. J. R. MCLAUGHLIN 1982 *Proceedings, Conference on the Theory of Ordinary and Partial Differential Equations, Dundee, Scotland,* March (W. N. Everitt and B. D. Sleeman, editors). Berlin: Springer-Verlag. Higher order inverse eigenvalue problems.
31. J. E. TAYLOR and M. P. BENDSØE 1984 *International Journal of Solids and Structures* **20**, 301–314. Modified min–max problems in structural optimization.
32. R. L. CRANE, K. E. HILLSTROM and M. MINKOFF 1980 *ANL*-80-64. Argonne National Laboratory, Argonne, Illinois. Solution of the general nonlinear programming problem with subroutine VMCON.

APPENDIX: INITIAL, FINAL AND TESTING VARIABLE VECTORS FOR THE FIRST CASE OF TABLE 1

Values of test data:

$x(1) = 0{\cdot}84702583,$ $x(12) = 0{\cdot}27460575\text{E} - 12,$
$x(2) = 70{\cdot}134849,$ $x(13) = 0{\cdot}00000000,$
$x(3) = 0{\cdot}50000000,$ $x(14) = 0{\cdot}80020908,$
$x(4) = 0{\cdot}00000000,$ $x(15) = 0{\cdot}66202768,$
$x(5) = 0{\cdot}35942968,$ $x(16) = 0{\cdot}28236713,$
$x(6) = 0{\cdot}67125385,$ $x(17) = -1{\cdot}0000000,$
$x(7) = 0{\cdot}89494491,$ $x(18) = -0{\cdot}28236713,$
$x(8) = 1{\cdot}0000000,$ $x(19) = 0{\cdot}66202768,$
$x(9) = 0{\cdot}89494491,$ $x(20) = 0{\cdot}80020908,$
$x(10) = 0{\cdot}67125385,$ $x(21) = 0{\cdot}74909186\text{E} - 12.$
$x(11) = 0{\cdot}35942968,$

Initial point:

$x(1) = 1{\cdot}0000000,$ $x(14) = 0{\cdot}92387953,$
$x(2) = 81{\cdot}000000,$ $x(15) = 0{\cdot}70710678,$
$x(3) = 0{\cdot}00000000,$ $x(16) = -0{\cdot}38268343,$
$x(4) = 0{\cdot}00000000,$ $x(17) = -1{\cdot}0000000,$
$x(5) = 0{\cdot}38268343,$ $x(18) = -0{\cdot}38268343,$
$x(6) = 0{\cdot}70710678,$ $x(19) = 0{\cdot}70710678,$
$x(7) = 0{\cdot}92387953,$ $x(20) = 0{\cdot}92387953,$
$x(12) = 0{\cdot}29322134\text{E} - 12,$ $x(21) = 0{\cdot}87966402\text{E} - 12.$
$x(13) = 0{\cdot}00000000,$

Value of objective function:

$$f = 118{\cdot}13502.$$

Values of equality constraints:

$g(1) = 0{\cdot}29960388,$ $g(4) = 0{\cdot}41391012\text{E} - 01,$
$g(2) = 34{\cdot}838632,$ $g(5) = 0{\cdot}68330718.$
$g(3) = 0{\cdot}23860437,$

Values of inequality constraints:

$$g(6) = -1{\cdot}0000000,$$
$$g(7) = 0{\cdot}00000000.$$

Final point:

$x(1) = 0{\cdot}84684129$, $x(12) = -0{\cdot}50121884\text{E}-04$,
$x(2) = 70{\cdot}134866$, $x(13) = -0{\cdot}50601379\text{E}-04$,
$x(3) = 0{\cdot}50033872$, $x(14) = 0{\cdot}80004009$,
$x(4) = -0{\cdot}50121884\text{E}-04$, $x(15) = 0{\cdot}66234831$,
$x(5) = 0{\cdot}35935882$, $x(16) = -0{\cdot}28235784$,
$x(6) = 0{\cdot}67115493$, $x(17) = -0{\cdot}99985175$,
$x(7) = 0{\cdot}89490786$, $x(18) = -0{\cdot}28235784$,
$x(8) = 1{\cdot}0002503$, $x(19) = 0{\cdot}66234831$,
$x(9) = 0{\cdot}89490786$, $x(20) = 0{\cdot}80004009$,
$x(10) = 0{\cdot}67115493$, $x(21) = -0{\cdot}50601377\text{E}-04$.
$x(11) = 0{\cdot}35935882$,

Values of objective function:

$$f = 0{\cdot}42440337\text{E}-06.$$

Values of equality constraints:

$g(1) = 0{\cdot}20934137\text{E}-05$, $g(4) = 0{\cdot}49168811\text{E}-07$,
$g(2) = 0{\cdot}41277232\text{E}-03$, $g(5) = 0{\cdot}14585115\text{E}-05$,
$g(3) = 0{\cdot}67061939\text{E}-06$,

Values of inequality constraints:

$$g(6) = -0{\cdot}49966128,$$
$$g(7) = -0{\cdot}50033872.$$

Comparison results:

No. of objective function calls = 198.
No. of constraints subroutine calls = 177.
No. of objective function gradient calls = 8.
No. of constraints gradient calls = 8.
Sum of constraints violation = $0{\cdot}41704403\text{E}-03$.
Norm of K–K–T vector = $0{\cdot}46118173\text{E}-02$.
Fortran STOP

APPENDIX B: NOMENCLATURE

a	depth of crack
$\underline{a}$	weighting factor on the cr and xc
a_i	ith generalized co-ordinate amplitude
A	cross-sectional area
b	half breadth of rectangular beam
c	$m-1$
cr	crack ratio $(=(d-h)/d=a/d)$
$\underline{cr}$	lower bound of the crack ratio
$\overline{cr}$	upper bound of the crack ratio
C_a	$C_a\hat{w}_a = w_a$

d	half depth of rectangular beam
E	Young's modulus of elasticity
$f(x, z)$	crack function
h	$d-a$
I	second moment of area of beam section
l	length of beam
T	numbers of measure station
Q	integrated crack function
m	stress magnification factor
M	numbers of modes that test information that is available
R	upper bound of value $[cr+\underline{a}xc]$
w_α	αth bending natural mode
$w_{t\alpha}$	test data corresponding αth bending mode
$\hat{w}_\alpha$	αth bending normal mode
$\hat{w}_{t\alpha}$	normalized test data corresponding αth bending mode
x_x	location of the crack
xc	$=x_c/l$, crack position
$\underline{xc}$	lower bound of the crack position
$\overline{xc}$	upper bound of the crack position
x_{tm}	mth out of T measure stations
ω_α	αth bending natural frequency
$\omega_{t\alpha}$	test data corresponding αth bending mode
$\delta_{\alpha\beta}$	the Kronecker delta
Φ	objective function
Ψ	upper bound on the objective function
ρ	density
ξ_α	natural frequency parameter
$\lambda, \Lambda, \mu, \Gamma$	Lagrange multipliers